CHAPTER IV
DIRECT CHITOSAN NANOSCAFFOLD FORMATION VIA CHITIN WHISKERS

Abstract

Chitosan nanoscaffold obtained directly from chitin whiskers is proposed. The structural analysis by nuclear magnetic resonance (^{1}H NMR) confirms that the alkaline treatment changes chitin whisker to chitosan nanoscaffold with as high as 98% degree of deacetylation. The micrographs from scanning electron microscope (SEM) and transmission electron microscope (TEM) confirm that the short fiber of chitin whiskers develop itself to be a network in nano-scale of chitosan or chitosan nanoscaffold. The increase in viscosity of chitosan nanoscaffold as compared to that of the chitin whiskers suggests that the scaffold network performs as a polymer bulk in the solution. The increases in surface area, pore volume, and pore size as studied by the Brunauer-Emmett-Teller (BET) gas adsorption inform the development of porous structure in chitosan. The well dispersion of nanoscaffold in the solution is easily controlled by the solvent polarity and salt concentration.

Keywords: Chitin whisker, Chitosan nanoscaffold, Nanomaterial

Introduction

Chitin-chitosan is a naturally occurring copolymer of β-(1-4)-2-acetamido-2-deoxy-β-D-glucose and β-(1-4)-2-amino-2-deoxy-β-D-glucose (Scheme 4.1) obtained from the shells of crustaceans, the cuticles of insects, or the cell walls of fungi and yeasts. The copolymer exhibits specific properties, especially bioactivity [1], biocompatibility [2], biodegradability [3], and non-toxicity [4] to afford the potential applications in pharmaceutical and biomedical fields. However, chitin-chitosan has its own limitation concerning its inertness, either its solubility or the reaction, due to the strong hydrogen bond network. For a chitin-based copolymer (degree of deacetylation less than 70%), only few solvents such as *N*,*N*–dimethylacetamide (DMAc) containing 5-10% LiCl, hexafluoroacetone, and

hexafluoro-2-propanol [5] are appropriate. In the case of chitosan, carboxylic and/or mineral acids are its good solvents and offer the simple materialization such as film casting [6] spray drying for beads or spheres [7], crosslinked gels or membranes [8-10].

Scheme 4.1

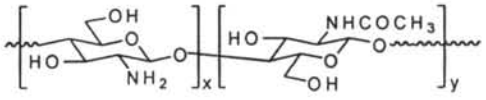

In the recent years, the scaffold has been known as an alternative materialization to obtain the product with nano/micro pores structure appropriate for the advanced applications, such as artificial extracellular matrices[11-13], micro-particles for drug delivery, and medical implants [14-18]. For chitosan, porous scaffolds were reported to be successfully prepared by the controlled lyophilization of chitosan solutions or gels [19,20], and by the electrospinning technique[21]. Although each method has its advantages, the use of acid and/or chemical reagents for solvents and crosslinkers and the dense precipitation of electrospun fibers raise questions about the chemical reagent contamination, scaffold porosity, and multi-steps preparation, etc.

Previously, Nair and Dufresne [22] reported about chitin whiskers via acid hydrolysis and proposed the use as reinforcing material for rubber. Herein, we report for the first time that chitosan nanoscaffold can be directly prepared from the chitin whisker. The preparation is simple and effective since it is a one-pot deacetylation and yields high amount of the chitosan nanoscaffold. Moreover, this scaffold is safe because no organic solvents or chemicals involved. The changing in morphology, i.e. from chitin nano-whisker to chitosan nanoscaffold, is also unique and important for further development when we consider the advanced and practical applications, especially the biomedical-based ones.

Experimental Section

Chemicals. Chitin flakes from shrimp shells were provided by Seafresh Chitosan (Lab) Company Limited, Thailand. Methanol and *iso*-propanol were purchased from Carlo Erba Reagenti, Italy. Sodium hydroxide, sodium chloride,

hydrochloric acid, acetic acid, and dimethylsulfoxide (DMSO) were obtained from Lab-Scan, Ireland. Hexafluoro-2-propanol (HFP) was provided by Central Glass Co., Ltd., Japan. Sodium trifluoroacetate (CF_3CO_2Na) was purchased from TCI-EP, Japan. Sodium acetate was obtained from Univar, Australia. All chemicals were analytical grade and were used without further purification.

Instruments and Equipment. Qualitative and quantitative Fourier transform infrared spectra were obtained from a Thermo Nicolet Nexus 670 with 32 scans at a resolution of 2 cm^{-1} in a frequency range of 4000-400 cm^{-1} using a deuterated triglycinesulfate detector (DTGS). Powder X-ray diffraction (XRD) patterns were recorded over a 2°-60° (2θ) by a RIGAKU RINT 2000 using CuKα as an X-ray source equipped with Ni filter and operating at 40 kV and 30 mA. TG-DTA thermogravimetric analyses were carried out using a Perkin-Elmer Pyris Diamond with a N_2 flow rate of 20 mL/min and a heating rate of 10 °C/min starting from 30 to 650 °C. ^1H NMR spectrum was recorded by a JNM-A500 500 MHz spectrometer at 70 °C using CD_3COOD/D_2O as a solvent. The morphology was investigated by using a JEOL JEM-1230 transmission electron microscope (TEM), and a JEOL JSM-5200 scanning electron microscope (SEM) at 80 and 15 kV, respectively. Particle sizes were observed by a Malvern Instruments Zetasizer Nano 75 light scattering instrument. The turbidity was determined by a Shimadzu UV-2550 UV-vis spectrophotometer. Surface area, pore volume, and pore size were measured by a Quantachrome Corporation Autusorb-1 gas sorption analyzer via the Brunauer-Emmett-Teller (BET) method applying the N_2 gas in the analyzer calibration and the liquid N_2 for the adsorbate. The sample was degassed overnight at 100 °C before measurement. The molecular weight of the chitosan nanoscaffold was measured by a Tohso HLC-8220 gel permeation chromatograph (GPC), equipped with RI detector and Tohso TSK-gel super H-RC and HM-N columns and the operating temperature was 40 °C. HFP containing 10 mM CF_3CO_2Na was used as an eluent with the flow rate of 0.2 mL/min and polymethyl methacrylate was used as a standard. The relative viscosity (η_r) was measured by a calibrated viscometer, Cannon-Ubbelohde (No. 2, A149), in 0.2 M CH_3COOH/0.1 M CH_3COONa aqueous solution at 30 ± 0.05 °C.

Procedures.

Chitin whiskers. Chitin whiskers were prepared as previously described by Nair and Dufresne [22] with some modifications. In brief, chitin, **1** (1.00 g), was treated in 3 N hydrochloric acid (100.0 mL) and stirred at 105 °C for 3 h to obtain the colloidal solution. The residues were collected after centrifugation and treated with hydrochloric for two times. Finally, the residues were dialyzed in distilled water until they were neutral and lyophilized to give chitin whiskers, **2**, for 86% yield (Scheme 4.2).

FTIR (KBr, cm^{-1}): 1661, 1624, and 1557 cm^{-1} (amides I and II).

Chitosan nanoscaffold. Compound **2** (20 mL, 2.45 g) was stirred in aq. NaOH (40% w/v, 100.0 mL) at 150 °C for 7 h and left at room temperature overnight. The residues were collected and the treatment was repeated for two times to result in the total alkaline treating time for 21 h. The crude product was dialyzed in distilled water until it was neutral and lyophilized to obtain, **3**, for 92% yield (Scheme 4.2).

FTIR (KBr, cm^{-1}): 1595 cm^{-1} ($-NH_2$). ^1H NMR (δ, ppm): 2.367 (NHAc), 3.435 (H2 of GlcN unit in chitosan), 4.023-4.255 (H2 of GlcNAc, and H3-H6 of pyranose ring), 4.9 (H1 of GlcNAc), 5.138 (H1 of GlcN).

Scheme 4.2

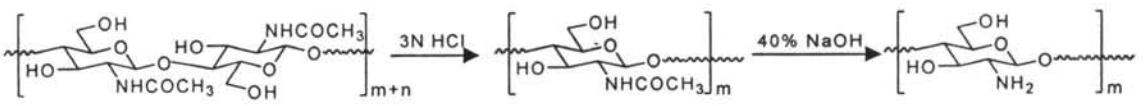

Chitin flake — Chitin whisker — Chitosan nanoscaffold

1 **2** **3**

Effect of the reaction time and temperature on the degree of deacetylation and molecular weight. The alkaline treating time was varied from 7 h to 28 h at 150 °C and the alkaline treating temperature was changed from 100 to180 °C for 21 h to observe how the degree of deacetylation and molecular weight changed. The degree of deacetylation (%DD) was calculated based on the ^1H NMR

spectrum considering the peak areas of the *N*-acetyl group (2.367 ppm) and the pyranose ring (4.023-4.255 ppm) using the following equation [23].

$$DD\ (\%) = \{1 - [(I_{CH_3} / 3) / (I_{\text{pyranose ring}} / 6)]\} \times 100$$

The effect of the reaction time and temperature on the degree of deacetylation was also quantitatively analyzed by FTIR and OPUS spectroscopic software version 2.0 based on the amide I band at 1656 cm^{-1} (-CONH-) and the internal standard C-O band at 895 cm^{-1} [24]. Relative viscosity (η_r) of **3** was used to simply trace how the molecular weight changed with the reaction time and temperature.

Colloidal Solution Stability and Effect of Solvent Polarity and Ionic Strength. Suspension of **3** in water (0.72 mg in 0.2 mL) was added to 25 mL of the purified solvents: distilled water, methanol, DMSO, and *iso*-propanol. The mixture was stirred for 1 min and left at room temperature overnight. Before examining the particle size by light scattering technique, the mixture was vigorously stirred for few minutes. Similarly, **3** was suspended in different salt concentration, i.e. NaCl 0.05, 0.1, 1.0, and 5.0 M. and the turbidity (1/%Transmittance) was observed at 650 nm in every 5 min for 20 min.

Results and Discussion

Chemical Structure Analysis.

Nair and Dufresne [22] reported the preparation of chitin whiskers by treating crab shells in 3 N HCl for 90 min. Here, the similar procedures were carried out to find that shrimp shell needed longer treating time, i.e. 3 h, to obtain the colloidal solution. The colloidal solution was lyophilized and the particles, **2**, were collected. The FTIR spectrum of **2** (Figure 4.1 (b)) demonstrates a typical type of chitin with the characteristic peaks at 1661, 1624, and 1557 cm^{-1} for amide I and amide II. Obviously, **2** shows the sharp characteristic peaks (Figure 4.1 (b)) as compared to the starting chitin flake (Figure 4.1 (a)), which might be due to the highly crystalline whisker. The morphology of **2** was further studied by TEM to conclude that **2** is in the whiskers form (see Morphological Studies).

Compound **2** was deacetylated in highly concentrated alkaline solution (40% aq.) to obtain **3**. As compared to **2** (Figure 4.1 (b)), **3** (Figure 4.1 (c)) shows a significant decrease in the peaks at 1661 and a new peak at 1595 cm^{-1} ($-NH_2$). The overall FTIR pattern of **3** is similar to that of chitosan flakes (Figure 4.1 (d)) confirming the successful deacetylation. Although **3** was expected to show the sharp peak, as it was derived from highly crystalline chitin whiskers of **2**, we found that **3** showed the broad bands, suggesting the increase in amorphous fraction (see Morphological Studies).

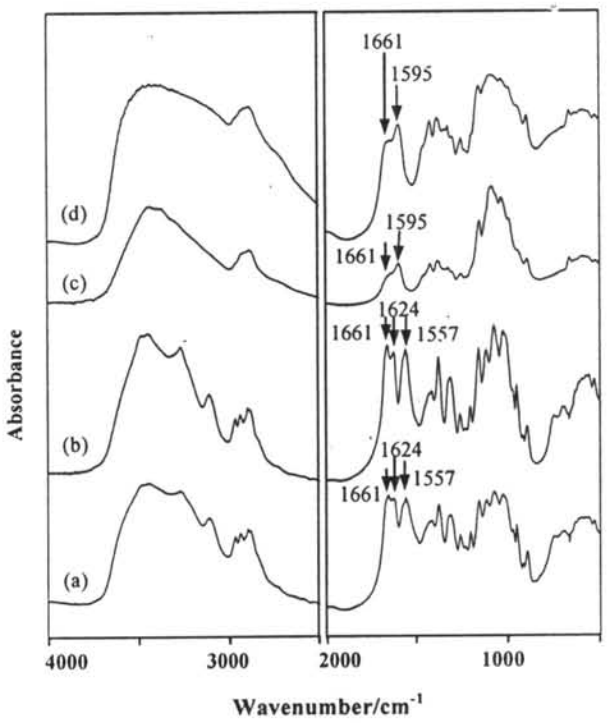

Figure 4.1 FTIR spectra of (a) chitin flakes, (b) **2**, (c) **3**, and (d) chitosan flakes (95%DD).

Studies on Degree of Deacetylation.

Figure 4.2 shows that the deacetylation of **2** gives **3** with a degree of deacetylation of 95% when the alkaline treatment was at 150 °C for 14 h [25]. The treatment of chitin whisker suspension in alkaline to obtain chitosan was quantitatively analyzed by ^1H NMR and FTIR. Figure 4.3 (A) shows an example of

FTIR curve fitting at 1656 cm^{-1} and 895 cm^{-1} when the alkaline treating temperature was varied. The peak ratio between these two peaks was plotted to confirm that the amide I band gradually decreased as the alkaline treating temperature was increased from 100 to 180 °C (Figure 4.3 (B)). Figure 4.3 (B) also shows how the results from ^{1}H NMR support the quantitative FTIR. It was found that the degree of deacetylation was as high as 98% for the alkaline treating temperature at 180 °C. When the alkaline treating temperature was fixed at 150 °C, the alkaline treating time for 7 h did not give the successful deacetylation as confirmed by FTIR. However, when the treating time was 14 h, the degree of deacetylation was suddenly increased to 95% (Figure 4.3(C)) as identified by ^{1}H NMR. Our preliminary works confirm that the alkaline solution should be as high as 40% for an effective deacetylation of the chitin whisker.

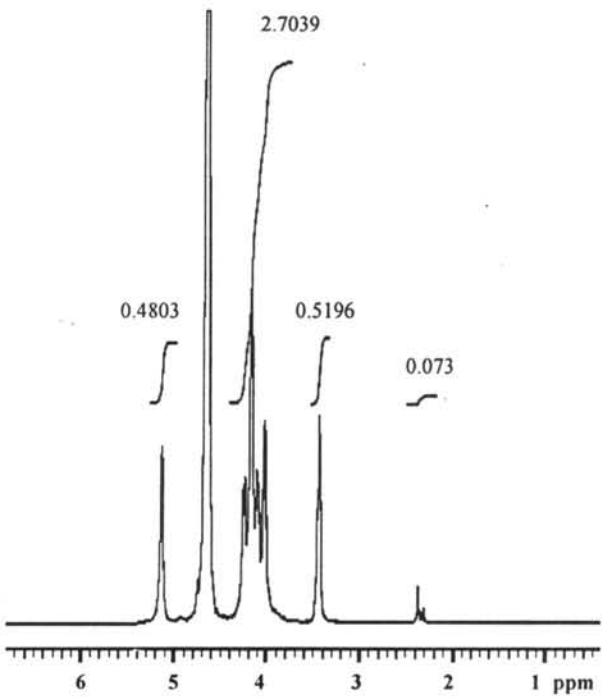

Figure 4.2 ^{1}H NMR spectrum of **3**.

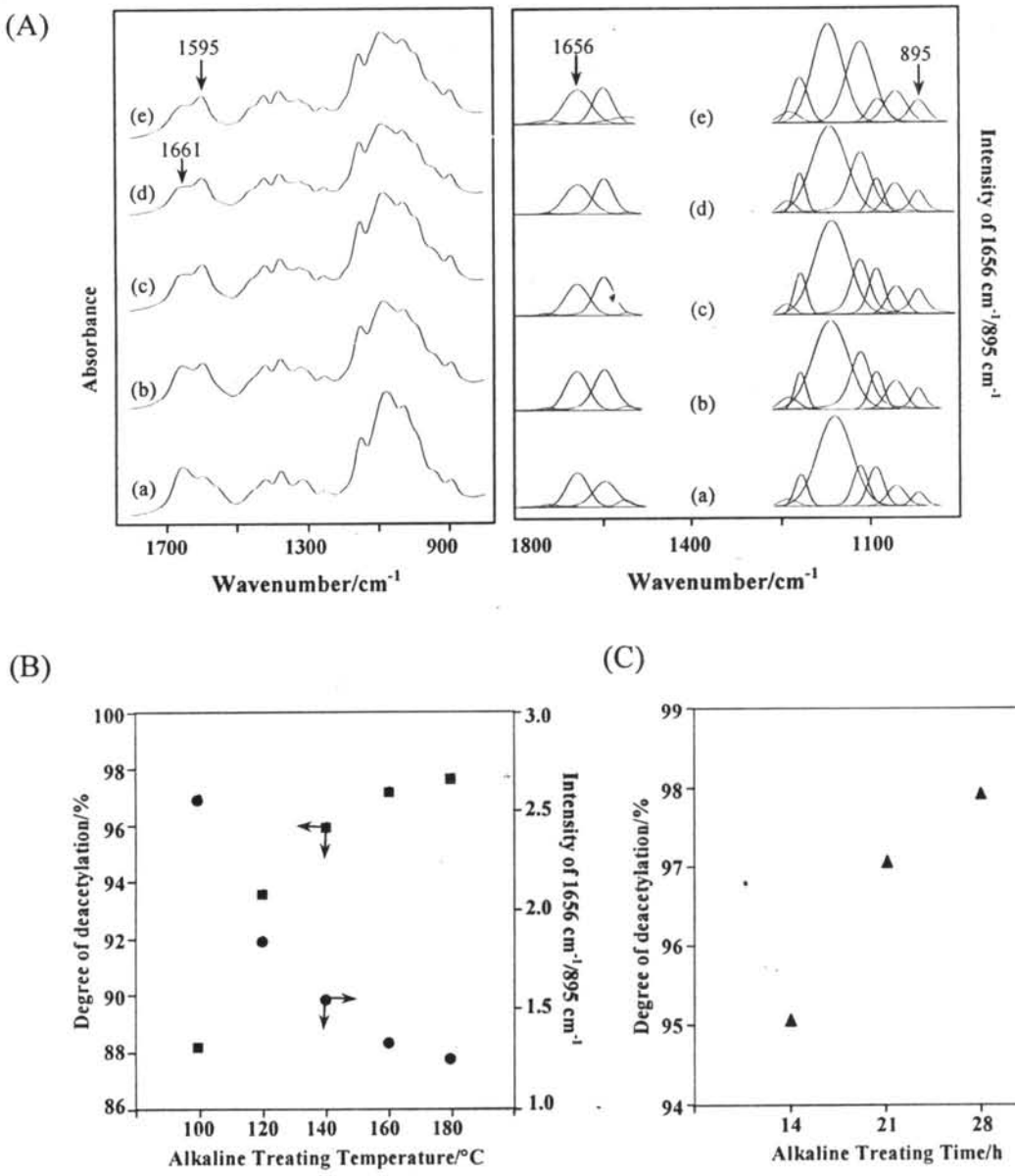

Figure 4.3 (A) FTIR spectra and the curve fitting of **3** under various alkaline treating temperatures for the alkaline treating time of 21 h: (a) 100°C, (b) 120°C, (c) 140°C, (d) 160 °C, and (e) 180°C; (B) quantitative analysis of **3** based on FTIR (•) and the degree of deacetylation of **3** resulted from ^{1}H NMR (■); (C) degree of deacetylation of **3** evaluated by ^{1}H NMR under various alkaline treating times for the alkaline treating temperature of 150°C.

Morphological Studies.

Considering the case of chitin, the specific treatment in hydrochloric acid solution changed the morphology of chitin as observed by WAXD (Figure 4.4 (a) and (b)). Here, the major peaks at 9° and 19° (2θ) are significantly sharp after chitin was hydrolyzed. The XRD pattern was relevant to the one reported by Nair et al. and this confirmed the crystalline structure of **2**. The observation by TEM confirmed that **2** is in highly crystalline of whisker form (see further discussion on Figure 4.5 (a)).

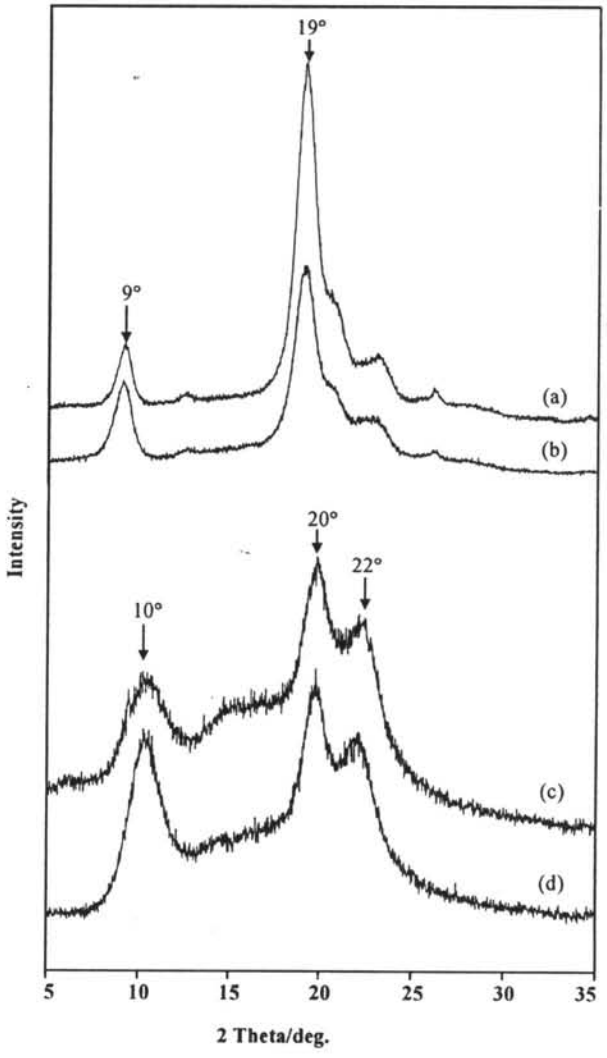

Figure 4.4 WAXD diffractograms of: (a) **2**, (b) chitin flakes, (c) **3**, and (d) chitosan flakes (95%DD).

As **3** was obtained from **2**, the similar crystalline structure was expected. Surprisingly, as shown in Figure 4.4, the WAXD pattern of **3** (curve (c)) is rather the broad along 2θ angles of 10°, 20°, and 22°. The peaks are broader than those of **2** (curve (a)) and even broader than that of the commercial chitosan flakes (curve (d)). This implied that the packing structure of **3** was changed from the tight packing to the amorphous morphology after alkaline treatment.

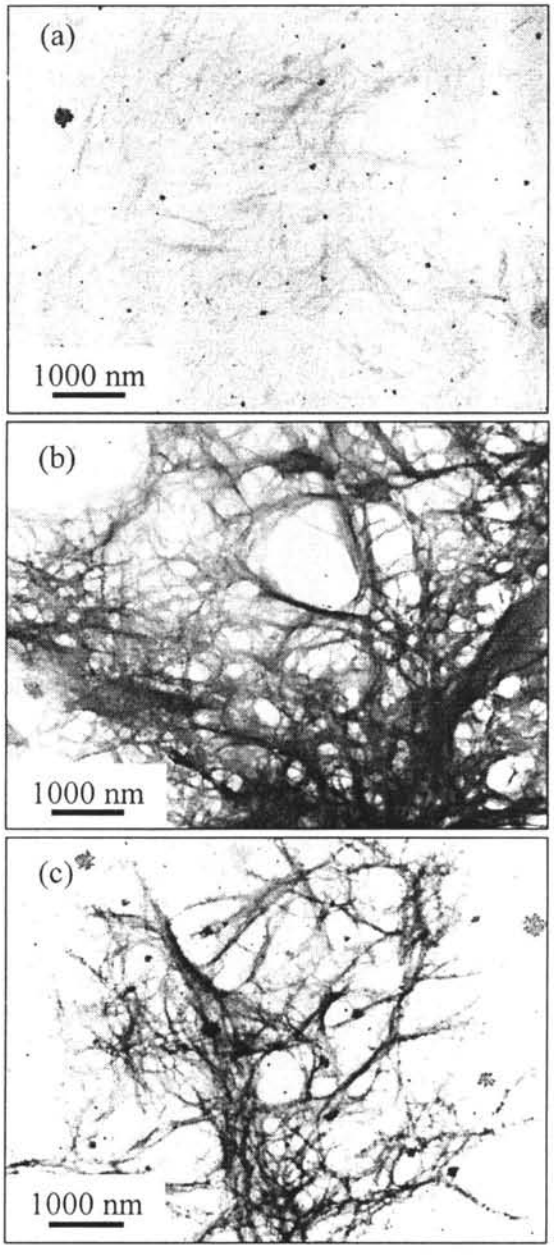

Figure 4.5 TEM micrographs of: (a) **2** in water, (b) **3** in water, and (c) **3** in DMSO.

Transmission electron microscopy (TEM) gives us the information to determine the morphology in details. Compound **2** gives a uniform needle, the so-called whisker, with a length of 200-560 nm, width of 18-40 nm, and an average aspect ratio of 18 (Figure 4.5(a)). It is important to note that the aspect ratio of **2** obtaining from shrimp shells is similar to that of the whisker from crab shells [22].

The observation of **3** by TEM clarifies that **3** is in fibrous form and each fiber is branching (Figure 4.5 (b)). Thus, it might not be appropriate to simply term **3** as nano-whisker. Taking this result with those from FTIR and WAXD into considerations, it can be concluded that the alkaline treatment changes the chitin nano-whisker to the chitosan nanoscaffold.

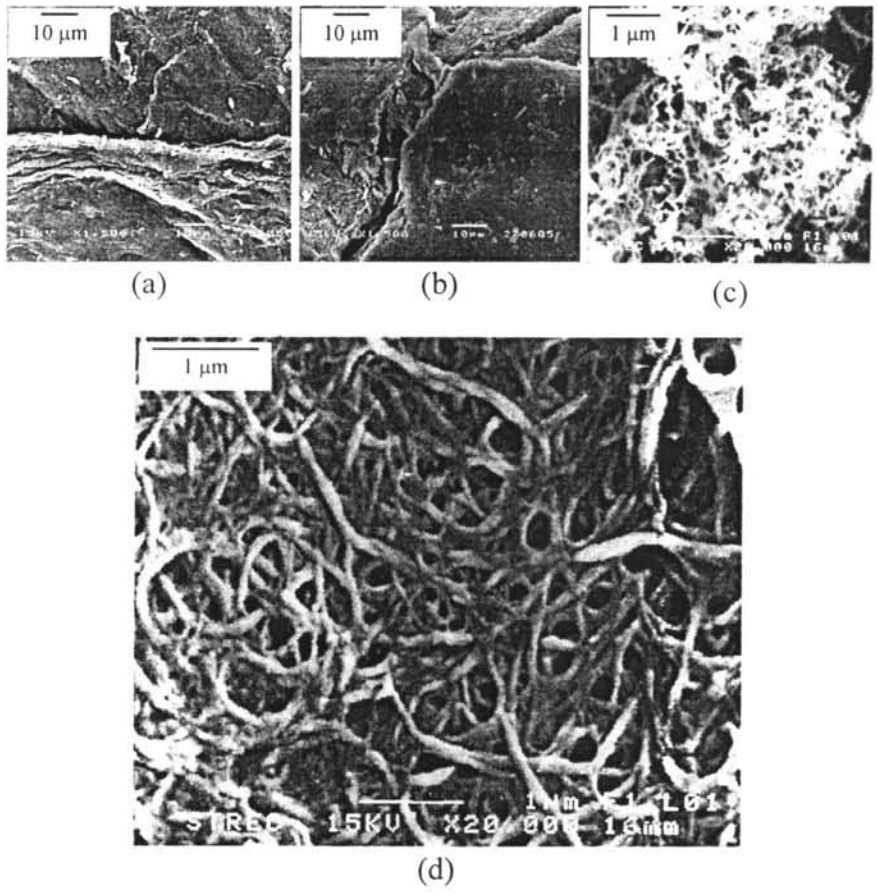

(a) (b) (c)

(d)

Figure 4.6 SEM micrographs at 15 kV of: (a) chitin flakes (× 1,500), (b) chitosan flakes 95% DD (× 1,500), (c) **2** (× 20,000), , and (d) **3** (× 20,000).

The scaffold structure was further confirmed by SEM. After **2** and **3** were lyophilized, the observation by SEM was carried out. The as-received chitin and chitosan flakes show a bulk material as indicated in Figure 4.6 (a) and (b). For **2**, the SEM micrograph shows the aggregation of whiskers (Figure 4.6 (c)) implying the packing of whisker after the lyophilization. When it comes to **3**, the packing was induced significantly to obtain a regular matrix structure as shown in Figure 4.6 (d). The fibrous network forms a porous structure with the pore diameter of ~ 200 nm.

Studies on Molecular Weight.

An attempt to clarify the chitin whisker and chitosan nanoscaffold in term of molecular weight was carried out. The GPC measurement was done in a specific condition using hexafluoro-2-propanol (HFP) as the solvent. As **3** was prepared by deacetylating **2** in highly concentrated alkaline solution, the chain scission to reduce molecular weight was expected. Surprisingly, it was found that **3** showed the molecular weight for 137,262 Da, whereas **2** was 62,838 Da. Considering the morphology of **3** as discussed above, the increase in molecular weight of **3** might come from the fact that **3** was in the scaffold structure. We suspected that when **3** was swelling with a scaffold network in HFP solvent, it might perform as a high molecular weight species or polymer bulk through the GPC column. In other words, the increase in molecular weight of **3** might be a kind of the apparent value due to the significant radius of gyration when chitosan was in a scaffold structure.

To confirm our speculation, the conditions in preparation of **3** with various alkaline treating temperatures and times were focused. The molecular weight of the samples was traced by simply taking the relative viscosity. As shown in Figure 4.7 (a) and (b), the increase in alkaline treating temperature and treating time result in the increase of viscosity. This might be due to the apparent viscosity of **3** as discussed in GPC result.

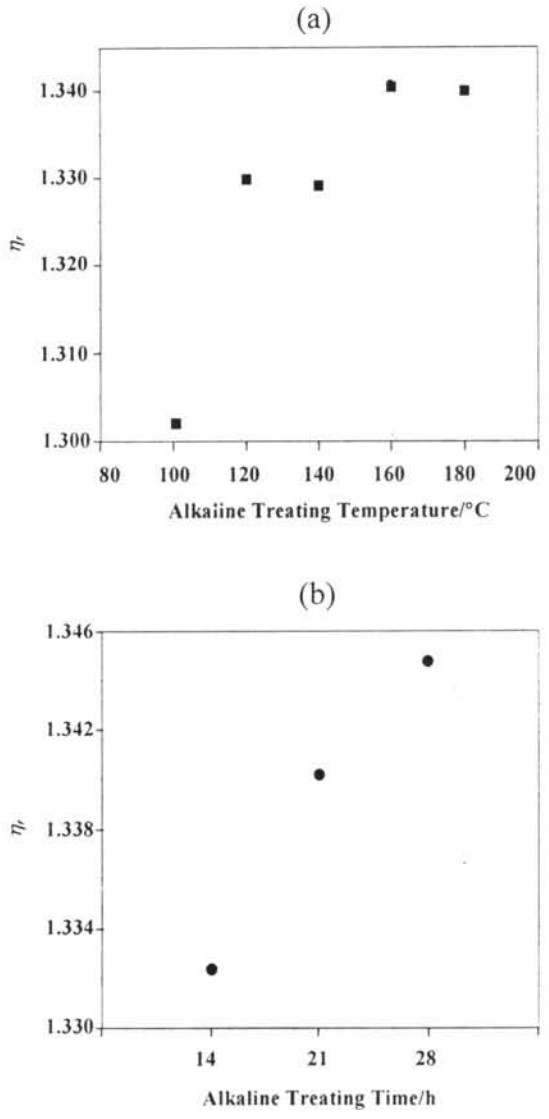

Figure 4.7 Relative viscosity of **3** by varying (a) alkaline treating temperature when the alkaline treating time was 21 h, and (b) alkaline treating time when the reaction temperature was 150°C.

Thermal Stability.

TGA studies under N_2 atmosphere were applied to identify the degradation temperature (T_d) and the amount of ash content (Table 4.1). In general, chitin-chitosan shows the ash content for 10-20% due to its strong hydrogen-bonded structure to induce incomplete combustion. It is expected that **2** would give lower

thermal stability than chitin as a result from the depolymerization, however, the degradation temperature and the ash content were found to be similar to those of chitin flakes.

Table 4.1 Degradation temperature (T_d) and ash content of chitin flakes, **2**, **3**, **3** (without lyophilization), and chitosan flakes 95%DD

Compound	T_d/°C	Ash content/%
Chitin flakes	387	16.28
2	387	18.57
3	308	25.67
3 (without lyophilization)	301	~1
Chitosan flakes 95%DD	309	35.30

It is important to note that when **3** was lyophilized, the product obtained was rather difficult to be well redispersed in the solvents. This implies that the drying step might initiate the recovery of inter and intramolecular hydrogen bond network among chitosan chain to result in the regular packing structure as demonstrated in SEM micrographs (Figure 4.6). As a result, **3** and chitosan flakes show the similar degradation temperature and the ash content (Table 4.1).

In order to avoid the repacking structure of **3**, the TGA study on **3** without lyophilization was carried out. Table 4.1 shows that **3** without lyophilization exhibited its T_d at 301 °C and the ash content for as less as 1%. This supports our speculation on the regeneration of the inter- and intramolecular hydrogen bond at a certain level after lyophilization.

Porosity of Nanoscaffold.

BET measurement was applied to evaluate the nanoscaffold for its porosity and surface area. As summarized in Table 4.2, chitin flakes give the surface area of 15.77 m^2/g, whereas **2** exhibits about twice that. The increase in surface area of **2** is relevant to the morphology as observed by SEM (Figure 4.6 (a) and (c)). The commercialized chitosan flakes give a surface area of 7.70 m^2/g. However, when it comes to **3**, the surface area over seven times that of the chitosan flakes (Table 4.2) and this supports the scaffold morphology in Figure 4.6 (d). Pore volume and pore

size are the other parameters to show the details about the scaffold structure. The increases in pore volume and pore size of **3** are as high as ~ 26 and ~ 4 times, respectively, compared to the chitosan flakes (Table 4.2). Pattison et al. [26] reported the PLGA scaffold with an average pore size diameter of ~ 215.0 μm, and a surface area ~ 441.25 m^2/g. Here, **3** shows the average pore size diameter at 15.8 nm (or 157.5 Å) denoting the nanometer level of the scaffold texture. The studies on cell adhesion and growth are in progress.

Table 4.2 Surface area, pore volume, and pore size of chitin flakes, **2**, **3**, and chitosan flakes 95%DD

Compound	**Surface area/(m^2/g)**	**Pore volume/(cc/g)**	**Pore size/Å**
Chitin flakes	15.77	0.03	64.47
2	34.59	0.04	40.69
3	55.75	0.22	157.50
Chitosan flakes 95%DD	7.70	0.01	43.20

Colloidal Solution Performance.

As nano-porous material allows an effective interaction with solvents, here, the effects of solvent, especially based on the ionic strength and polarity, were studied. It should be noted that the treatment of chitin whiskers in the strong alkaline solution followed by dialysis in water brought about the colloidal solution of **3** in water. This implies the surface hydrophilicity and its interaction with water molecules. A good ion dissociation solution of sodium chloride was chosen as a model system to study on an effect of ionic strength to the colloidal formation. Here, a certain concentration of sodium chloride solution was added to observe how ionic strength in the solution affected the colloidal formation. Figure 4.8 shows the dispersion ability of **3** as evaluated by the turbidity (1/%Transmittance). At initial stage (t = 0), an increase in sodium chloride concentration (from conditions (b) to (e)) induces the increase in turbidity. In other words, the increase in salt concentration enhances the dispersion or swelling of **3**. This might come from the effect of the salt concentration obstructing the interaction between each fiber in

nanoscaffold. However, when the time passed, the conditions (b) - (d) show a significant decrease in turbidity (Figure 4.8) implying the aggregation of **3**. For condition (e), where the salt concentration is almost saturated, the ionic strength might inhibit the aggregation of **3** allowing the dispersion stability to maintain the colloidal solution state for months.

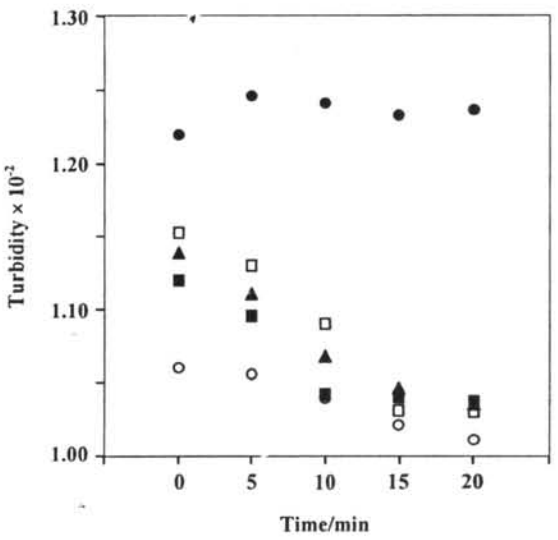

Figure 4.8 Turbidity of **3** in (a) distilled water (○), (b) NaCl 0.05 M (■), (c) NaCl 0.1 M (▲), (d) NaCl 1.0 M (□), and (e) NaCl 5.0 M (●).

The interaction of **3** with a series of solvents having different polarities was extensively studied. It was expected that the polarity might be another factor to control the swelling of scaffold. Table 4.3 reveals the effect of the solubility parameter (δ) on the particle size of **3** as determined by light scattering technique. The δ values for water, methanol, DMSO, and *iso*-propanol are 23.4, 14.5, 12, and 11.5 $(cal.cm^{-3})^{0.5}$, respectively [27]. It was found that the particle size of **3** was increased when the solubility parameter increased. The particle size was as high as 2000 nm when **3** was in water suggesting the good swelling of **3** in aqueous. Here, the TEM technique was applied to observe how the solvent contributed the texture of scaffold. Figure 4.5 shows the morphology of **3** in water (Figure 4.5 (b)) and in DMSO (Figure 4.5 (c)). It was clearly observed that the scaffold was significantly

deformed in DMSO (Figure 4.5 (c)). This indicates the effect of the solvent on the scaffold morphology.

Table 4.3 Particle size of **3** in water, methanol, DMSO, and iso-propanol

Solvent	**Solubility parameter/(cal.cm^{-3})$^{0.5}$**	**Average particle size/nm**
Water	23.4	2124.4
Methanol	14.5	519.4
DMSO	12.0	226.6
Iso-Propanol	11.5	533.1

Conclusions

Chitosan in nanoscaffold structure was successfully prepared via a one pot deacetylation of chitin whisker. The branching of each chitin whisker initiated the scaffold formation as observed by TEM. The lyophilization induced the packing of nanoscaffold to be a regular network as evidenced by SEM. The scaffold structure of chitosan also exhibited the increase in the molecular weight and viscosity as compared to that of chitin whisker starting material. The studies on the dispersion in solvents with different solubility parameters confirmed that water can be used as a well dispersed system for chitosan nanoscaffold. The aggregation of the scaffold could also be controlled by the high ionic strength solvent.

Acknowledgements.

The authors gratefully acknowledge the partial financial support from the Royal Golden Jubilee Ph. D. Program, the Thailand Research Fund, and the National Research Council of Thailand (NRC 12/2548). One of the authors (S. C.) is indebted to the generous contribution of the Hitachi Scholarship Foundation to the continuation of his research activities. The authors extend their appreciation to the Seafresh Chitosan (Lab) Company limited, Thailand for chitin and chitosan materials.

References

[1] Dumitriu S, Popa MI, Cringu A, Stratone A. Colloid Polym Sci 1989;267:595.

[2] Hirano S, Seino H, Akiyama Y, Nonoka I. Polym Mater Sci Eng 1988;59:897.

[3] Yamamoto H, Amaike M. Macromolecules 1996;30:3936.

[4] Chandy T, Sharma CP. Biomaterials 1992;13:949.

[5] Kurita K. Prog Polym Sci 2001;26:1921.

[6] Bégin A. Calsteren MRV. Inter J Bio Macromol 1999;26:63.

[7] Hoagland PD, Parris N. Ind Eng Chem Res 1997;36:3631.

[8] Pellegrino JJ, Geer S, Maegley K, Rivera R, Steward D, Ko M. Chitin/Chitosan Membranes: Amino acid and Polypeptide Separations. Proceedings of Biochemical Eng VI, W.E. Goldstein, D. Dibiasio, and H. Pedersen, Ann. N.Y. Acad. Sci 1990;589.

[9] Zeng X, Ruckenstein E. Ind Eng Chem Res 1996;35:4169.

[10] Mao JS, Liu HF, Yin Y, Yao KD. Biomaterials 2003;24:1621.

[11] Fields GB, Lauer JL, Dori Y, Forns P, Yu YC, Tirrell M. Biopolymers 1998;47:143.

[12] Ma J, Wang H, He B, Chen J. Biomaterials 2001;22:331.

[13] Adekogbe I, Ghanem A. Biomaterials 2005;26:7241.

[14] Jia H, Zhu G, Vugrinovich B, Kataphinan W, Reneker DH, Wang P. Biotechnol Prog 2002;18:1027.

[15] Khil MS, Cha DI, Kim HY, Kim IS, Bhattarai N. J Biomed Mater Res 2003;67B:675.

[16] Xu CY, Inai R, Kotaki M, Ramakrishna S. Biomaterials 2004;25:877.

[17] Min BM, Lee G, Kim SH, Nam YS, Lee TS, Park WH. Biomaterials 2004;25:1289.

[18] Guo T, Zhao J, Chang J, Ding Z, Hong H, Chen J, et al. Biomaterials 2006;27:1095.

[19] Madihally SV, Matthew HWT. Biomaterials 1999;20:1133.

[20] Berger J, Reist M, Mayer J, Felt O, Peppas N, Gurny R. Eur J Pharm Biopharm 2004;57:19.

[21] Bhattarai N, Edmonson D, Veiseh O, Matsen FA, Zhang M. Biomaterials 2005;26:6176.

[22] Nair KG, Dufresne A. Biomacromolecules 2003;4:666.

[23] Sashiwa, H. Shigemasa, Y. Cabohyd Polym 1999; 39: 127.

[24] Van de Velde, K, Kiekens, P. Cabohyd Polym 2004; 58: 409.

[25] Degree of deacetylation (%) = {1 – [(0.073 / 3) / (2.7039 / 6)]} × 100 = 94.60%.

[26] Pattison MA, Wurster S, Webster TJ, Haberstroh KM. Biomaterials 2005;26:2491.

[27] Grulke EA. Polymer Handbook: John Wiley & Sons, 1989.